Global NEST Journal, Vol 17, No 4, pp 756-770, 2015

APPLICATION OF RESPONSE SURFACE METHODOLOGY FOR ULTRASOUND-ASSISTED RAPID ADSORPTION OF MESO-TETRAKIS(4-SULFONATOPHENYL) PORPHYRIN BY COPPER NANOWIRE-LOADED IN ACTIVATED CARBON: CHARACTERIZATION, EQUILIBRIUM AND KINETIC MODELING

BAHRAMIAN M.
KARIMIPOUR G.*
GHAEDI M.*
ASFARAM A.
NASIRI AZAD F.
BAZRAFSHAN A.A.

Chemistry Department, Yasouj University
Yasouj 75918-74831, Iran

Received: 23/08/2015
Accepted: 27/10/2015
Available online: 04/11/2015

*to whom all correspondence should be addressed:
e-mail: ghkar@yu.ac.ir; m_ghaedi@mail.yu.ac.ir

ABSTRACT

The combined ultrasonic assisted/nanoparticle based procedure was described for an economical and rapid removal of meso-tetrakis (4-sulfonatophenyl) porphyrin (TSPP) by copper nanowires loaded on activated carbon (Cu-NW-AC). The synthesized Cu-NW-AC was investigated by scanning electron microscopy (SEM) and X-ray diffraction (XRD). Response surface methodology (RSM) combined with central composite design (CCD) give useful information about the individual contribution and interaction amoung variables correspound to above adsorption. In CCD, the effects of variables in the following range, pH (X_1: 5.0-7.0), adsorbent dosage (X_2: 0.021-0.051 g), initial TSPP concentration (X_3: 3-15 mg l^{-1}) and ultrasound time (X_4: 2-10 min.) was investigated to obtain maximum adsorption effeciency. The experimental data were subsequently fitted to a second-order polynomial equation using multiple regression analysis by appropriate statistical methods. According to the results, the optimum adsorption conditions were found to be Cu-NW-AC = 0.04 g, TSPP = 6 mg l^{-1}, pH = 5.5 and ultrasound time = 8.0 min. The experimental extraction yield under optimal conditions was found to be 97.60% which confirmed by three replicate at optimum conditions leading to removal percentage of 98.16%. The adsorption equilibrium isotherm and kinetic models investigation revealed the suitability of Langmuir isotherm and pseudo-second-order model for best predication of experimental data. Maximum monolayer capacity (Q_m) calculated from Langmuir model was found to be 26.385 mg g^{-1}.

Keywords: Activated carbon; Adsorption; Copper nanowires; Meso-Tetrakis(4-sulfonatophenyl)porphyrin (TSPP); Response surface methodology.

1. Introduction

Porphyrins are a group of tetrapyrrole compounds that are ubiquitous in biology and are largely responsible for pigments in everything from chlorophyll in plants to hemoglobin in blood (Meunier, 1992). Synthetic porphyrins and metalloporphyrins have featured widely in recent research due to their rich chemistry, making them promising candidates for a large number of applications such as catalysis, nonlinear optics, enzyme models, sensors and molecular electronics (Feiters *et al.*, 2000; De Montellano,

Bahramian M., Karimipour G., Ghaedi M., Asfaram A., Nasiri Azad F. and Bazrafshan A.A. (2015), Application of response surface methodology for ultrasound-assisted rapid adsorption of meso-tetrakis(4-sulfonatophenyl) porphyrin by copper nanowire-loaded in activated carbon: characterization, equilibrium and kinetic modeling, *Global NEST Journal*, **17**(4), 756-770.

2005; Seufert *et al.*, 2011) as well as their biological and medicinal activities (Granville *et al.*, 2001; Vicente, 2001).

However, these materials are hazardous to human health and the environment, and thus necessitate their proper management, waste minimization, and eventual disposal. For instance, high levels of porphyrins are toxic to the brain, nerves, skin and gastrointestinal tract. Moreover, some porphyrin metabolites are toxic and when accumulation in the body cause abnormal sensitivity to light, pain and nerve damage including paralysis (Chow and Chow, 2006).

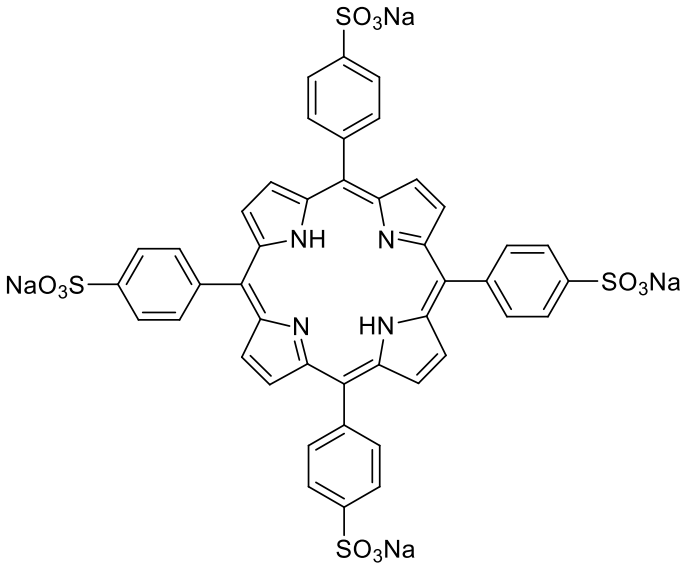

Scheme 1. Structure of TSPP

On the other hand, water soluble porphyrins are more hazardous than others becaouse they are easily soluble in water and consequences for environmental risk assessment.Therefore, it is important to find an effective method for their removal from real samples. Meso-tetrakis(4-sulfonatophenyl)porphyrin (TSPP) (Scheme 1) as a biomimetic pigment is soluable in water due to the presence of four sulfonate groups located on the phenyl rings of the porphyrin. It is belived that TSPP is toxic to humans (LD50 = 0.5 mmol/kg) (Place *et al.*, 1992). So, it should be considered as a pollutant agent and require to extend new method for their efficint and quantitive removal from water media. In this regard versatile approaches like photodegradation based on nanomaterials for common pollutants has been reported (Xue *et al.*, 2015). Amongst, adsorption based procedure is highly recommended. This procedure is a well-established technique widely utilized for wastewater treatment due to the advantages such as high efficiency, capacity and large scale ability with generable adsorbents (Duran *et al.*, 2009; Ghaedi *et al.*, 2012a; Ghaedi *et al.*, 2012c). Activated carbon (AC) is used as a global adsorbent for adsorption of pollutants from wastewater due to their extended surface area, non-toxicity, low cost, porous structure, fast adsorption kinetics, large adsorption capacities, and high abundance. These advantages make it suitable for use as adsorbent and/or support for loading nano-structure materials (Ghaedi *et al.*, 2012b) and extensively enhance their subsequent application in various fields. In this technique, application of nano scale materials with high surface area elevates the removal percentage and adsorption capacity of AC-based adsorbent.

The literature review shows that no investigation is available for removaling of anionic water-soluble porphyrins.

In this study, Cu-NWs-AC as low-cost, high surface area and eco-friendly adsorbent was prepared, characterized and efficiently used for the removal of TSPP from aqueous solutions, while influence of variables such as pH, ultrasound time, initial TSPP concentration and adsorbent dosage were investigated and optimized by response surface methodology (RSM). Design and analysis of experiments (DOE) have

been widely used in planning, analyzing, and running experiments in different areas, such as wastewater treatment, food analysis, material production and medication intake, which helps to minimize cost and time. The application of DOE in wastewater industries has increased because it enables efficient data collection and reduces error by excluding non-significant factors from the experiment, as well as increasing the accuracy of the results to the target range. Moreover, adsorption isotherms and kinetics parameters were also evaluated and reported.

2. Experimental

2.1. Materials and apparatus

$CuSO_4 \cdot 5H_2O$, NaOH, HCl, ethylene di-amine ($C_2H_8N_2$) and hydrazine (N_2H_4) were analytical reagent grade and purchased from Merck (Darmstadt, Germany) and used without further purification. The stock solution (100 mg l^{-1}) of TSPP was prepared by dissolving 0.01 g of solid TSPP in 100 ml double distilled water and the working concentrations daily were prepared by its suitable dilution. The pH measurements were carried out using a digital pH meter (Ino Lab pH 730, Germany) and the TSPP concentrations were determined using Jasco UV-Vis spectrophotometer model V-530 (Jasco, Japan) at a wavelength of 414 nm for porphyrin. An ultrasonic bath with heating system (Tecno-GAZ SPA Ultra Sonic System, 130 W- 40 KHz, Bologna, Italy) was used for the ultrasound-assisted adsorption procedure. The samples were characterized by powder X-ray diffraction (XRD) pattern, using Philips Analytical X-Ray, Netherlands operating with $Cu_{K\alpha}$ radiation for 2θ values over 10-80°. The morphology of the prepared composite nanowires was characterized by scanning electron microscopy (SEM, Hitachi S4160, Tokyo, Japan).

2.2. Synthesis of meso-tetrakis (4-sulfonatophenyl)porphyrin (TSPP)

In the first step, *meso*-tetraphenylporphyrin (TPP) was prepared using freshly distilled pyrrole and benzaldehyde (Zhou *et al.*, 2007). M*eso*-tetrakis(4-sulfonatophenyl)porphyrin (TSPP) was prepared by suffocation of the prepared TPP (2 g) with concentrated H_2SO_4 (50 ml). The crude product was purified according to the procedure of Tsutsui (Srivastava & Tsutsui, 1973) to yield 60% pure TSPP. The purity of TSPP was confirmed by ultraviolet-visible (UV–Vis) and IR spectroscopy. The UV–Vis spectrum of TSPP (H_2O, pH 10.0) showed five peaks at 414 (Soret band), 513, 552, 581 and 633 nm. The IR spectrum of TSPP (KBr) show wed four strong bands at 1218, 1188, 1125 and 1039 cm^{-1} due to sulfonic acid.

2.3. Preparation of copper nanowires-AC (Cu-NWs-AC)

Cu nanowires were synthesized according to Zeng and coworkers (Ghaedi *et al.*, 2015a). Aqueous solution of NaOH (30 ml 15 mol L^{-1}) and $CuSO_4 \cdot 5H_2O$ (1.0 ml, 0.10 mol l^{-1}) were added to a glass reactor. Then, ethylenediamine (2.0 ml; 99 wt %) and hydrazine (1.0 ml; 35 wt %) were added sequentially to this reactor, followed by a thorough mixing of all reagents. The reactor was then placed in an ultrasound at 60°C for 2h, leading to the formation of Cu NWs. 50 ml of the freshly prepared Cu NWs solution was then added to activated carbon (3.0 g) in a 100 ml flask under ultrasound at 60°C for 1 h and the mixture was stirred for 12 h. The suspension was filtered off and the prepared Cu-NWs-AC was washed with water and dried at 95-100 °C for 12 h.

2.4. Batch adsorption experiment

The sonochemical adsorption experiment was undertaken as follows: 50 ml of 6 mg l^{-1} TSPP was mixed thoroughly with 0.04 g of Cu-NWs-AC at pH = 5.5 at room temperature for 8 min ultrasound. Finally, the sample was centrifuged and the solution was analyzed for the final TSPP concentration via UV-Vis spectrophotometry at 414 nm. The efficiency of the porphyrin adsorption was determined at different experimental condition according to CCD method (Asfaram *et al.*, 2015a; Bagheri *et al.*, 2015). The porphyrin removal percentages were calculated using the following equation (Jamshidi *et al.*, 2016):

$$\%\text{TSPP removal} = \frac{(C_0 - C_t)}{C_0} \times 100\% \quad (1)$$

where C_0 (mg l^{-1}) and C_t (mg l^{-1}) is the concentration of target at initial and after time t, respectively. The adsorption capacity of the TSPP was calculated from the following equation (Nasiri Azad *et al.*, 2015):

$$q_e = \frac{(C_0 - C_e)V}{W} \quad (2)$$

where C_0 (mg l^{-1}) and C_e (mg l^{-1}) are the initial and equilibrium concentrations of TSPP in solution, respectively. V (l) is the volume of TSPP solution and W (g) is the mass of the Cu-NWs-AC.

2.5. Experimental proceedings and design

The simultaneous optimization is superior to conventional one variable at a time in term of requirement of lower number of experiments. Therefore, it is possible to design cheaper protocol that provide useful information about influence of each variable in individual situation and/or interaction affecting (Asfaram *et al.*, 2015a).

Table 1. Experimental factors and levels in the central composite design

Factors				Levels				
				Low (-1)	Central (0)	High (+1)	-α	+α
X_1: pH				5.5	6.0	6.5	5.0	7.0
X_2: Adsorbent dosage (g)				0.028	0.036	0.043	0.021	0.051
X_3: Initial TSPP concentration (mg l^{-1})				6.0	9.0	12.0	3.0	15.0
X_4: Ultrasound time (min)				4.0	6.0	8.0	2.0	10.0
	Factors				R% TSPP			
Run	X_1	X_2	X_3	X_4	R% (Exp.)[a]	R% (Pre.)[b]	Residual	
1	6.0	0.036	9.0	6.0	49.00	46.67	2.33	
2	5.5	0.043	6.0	4.0	90.00	90.94	-0.94	
3	5.0	0.036	9.0	6.0	76.00	75.00	1.00	
4	6.5	0.043	6.0	8.0	84.00	84.94	-0.94	
5	6.0	0.036	9.0	10.0	78.00	77.00	1.00	
6	6.0	0.021	9.0	6.0	42.00	40.88	1.13	
7	6.0	0.036	9.0	6.0	46.00	46.67	-0.67	
8	6.0	0.036	9.0	6.0	45.01	46.67	-1.67	
9	5.5	0.043	12.0	8.0	56.00	56.94	-0.94	
10	6.0	0.051	9.0	6.0	69.00	68.13	0.88	
11	6.0	0.036	3.0	6.0	96.00	95.00	1.00	
12	6.0	0.036	9.0	6.0	44.35	46.67	-2.32	
13	5.5	0.028	12.0	8.0	40.00	41.06	-1.06	
14	6.5	0.028	12.0	4.0	30.00	31.06	-1.06	
15	7.0	0.036	9.0	6.0	51.00	50.00	1.00	
16	6.0	0.036	9.0	6.0	49.00	46.67	2.33	
17	6.5	0.043	12.0	4.0	36.00	36.94	-0.94	
18	5.5	0.028	6.0	4.0	70.00	71.06	-1.06	
19	6.5	0.028	6.0	8.0	71.00	72.06	-1.06	
20	6.0	0.036	9.0	2.0	49.00	48.00	1.00	
21	6.0	0.036	15.0	6.0	32.00	31.00	1.00	

[a] R% (Exp.): experimental value; R% (RSM): predicted by RSM

In this work, the CCD was applied for simultaneous optimization of the ultrasonic assisted rapid adsorption of TSPP onto Cu-NWs-AC as a green and safe nano structure sorbent. A five-level CCD was used based on the variables including pH (X_1), adsorbent dosage (g, X_2), initial TSPP concentration (mg l^{-1}, X_3) and ultrasound time (min, X_4) in randomized fashion to minimize the effects of the uncontrolled factors. The

design matrix and respective responses values for TSPP removal is shown in Table 1. In this technique, a second-order polynomial equation will obtain that generally has quadratic equation (Fayyazi *et al.*, 2015).

$$y=\beta_0+\sum_{i=1}^{4}\beta_i x_i+\sum_{i=1}^{4}\sum_{j=1}^{4}\beta_{ij}x_i x_j+\sum_{i=1}^{4}\beta_{ij}x_i^2 \quad (3)$$

where y is the predicted response (removal percentage of TSPP); Xi's are the independent variables that are known for each experimental run. The parameter β_0 is the model constant; β_i's are the linear coefficients; β_{ii}'s are the quadratic coefficients and β_{ij}'s are the interaction coefficients (Ghaedi *et al.*, 2015c). The analyses of variance (ANOVA) correspond to CCD give useful information about significance levels of parameters. The graphical interpretation of tri-dimensional plots of response versus two factors give information about dependency of signal to each variable as single or binary contribution (interaction).

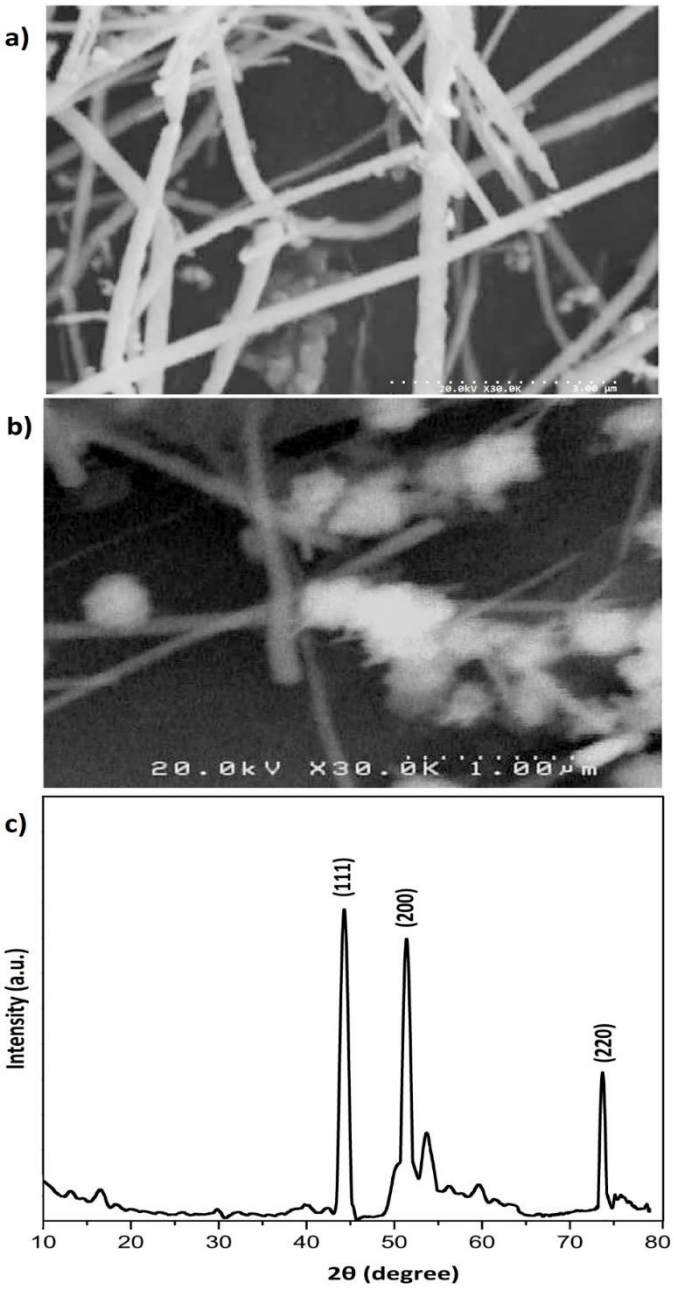

Figure 1. (a) and **(b)** SEM images of Cu NWs and **(c)** XRD patterns of Cu NWs-AC

3. Results and discusion

3.1. Characterization of adsorbent

The SEM image of the Cu-NWs (Fig. 1 (a) and (b)) confirm that homogeneous and smooth surface of AC modified by large quantity of well-dispersed Cu NWs with average diameter of ~ 81 nm (calculated from 20 nanowires randomly selected from the SEM image). The lengths of the nanowires vary from tens to hundreds of micrometers. XRD analysis (Fig. 1c) reveals (111), (200) and (220) crystal planes which is in good agreement with card number of JCPDS 65-9743 and proves the face-centered cubic structure of Cu NWs.

3.2. CCD results for adsorption of the porphyrin

In the CCD, the plan of experiments was run in a random manner in order to minimize the effect of uncontrolled variables. Table 1 show the independent variables (pH, X_1), adsorbent dosage (g, X_2), initial TSPP concentration (mg l^{-1}, X_3) and ultrasound time (min, X_4) at five levels according to previous reports (Roosta *et al.*, 2015).

21 experiments were performed for the optimization of the adsorption procedure according to the CCD and their responses are presented in Table 1.

Table 2 presents the results of ANOVA and respective regression coefficients based on the judgment of $p < 0.05$. The lack of fit (LOF) as data variation around the fitted model considered as criterion for judgment about adequacy of obtained model. This phenomenon emerged from elimination of effects concern to the additional higher-order terms. The failure of theoretical model for the best prediction of real LOF was 0.300 that suggest the high ability and applicability of theoretical model for accurate and repeatable prediction of real behavior of experimental data. The quality of fitting of the polynomial model equation was expressed by the coefficient of determination (R^2=0.9953 and adjusted R^2=0.9844).

Table. 2. Analysis of variance (ANOVA) for R% of TSPP.

Factor	SS	Degrees of freedom	MS	F	p
X_1	312.500	1	312.500	64.230	0.00131
X_1^2	393.031	1	393.031	80.782	0.00085
X_2	742.563	1	742.563	152.623	0.00025
X_2^2	96.146	1	96.146	19.762	0.01129
X_3	2048.000	1	2048.000	420.938	0.00003
X_3^2	418.253	1	418.253	85.966	0.00075
X_4	420.500	1	420.500	86.428	0.00074
X_4^2	393.031	1	393.031	80.782	0.00085
X_1X_2	36.125	1	36.125	7.425	0.05272
X_1X_3	68.063	1	68.063	13.989	0.02012
X_1X_4	39.062	1	39.062	8.029	0.04718
X_2X_3	15.125	1	15.125	3.109	0.15265
X_2X_4	1.125	1	1.125	0.231	0.65573
X_3X_4	14.063	1	14.063	2.890	0.16434
Lack of Fit	16.062	2	8.031	1.651	0.30013
Pure Error	19.461	4	4.865		
Total SS	7610.979	20			
Quality of quadratic model based on R^2 and standard deviation					
Response	SD	mean	CV%	Adequate precision	R^2
R% TSPP	2.43	57.30	4.25	31.12	0.9953

The large adjusted R^2 values indicate a good relationship between the experimental data and the fitted model. The value of the "adequate precision" for this model is 31.12 and support sufficiency of model and empirical equation for accurate and repeatable prediction of response.

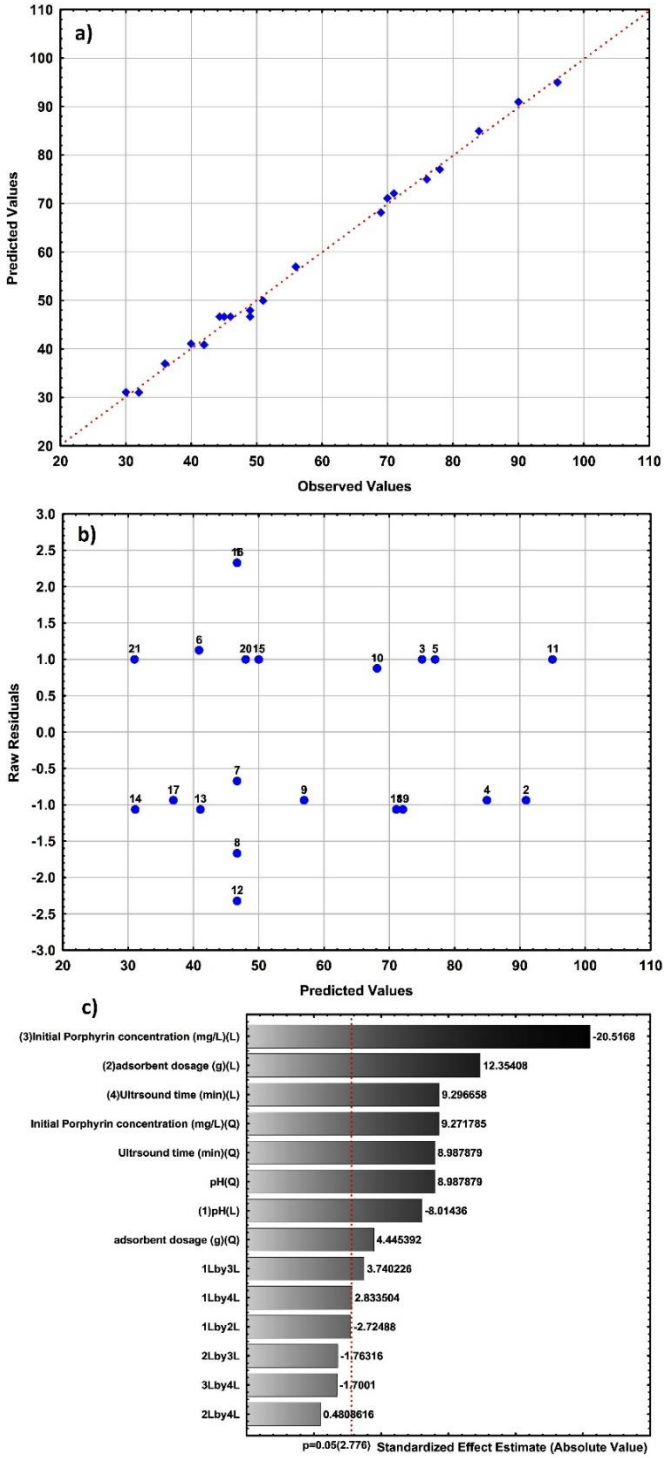

Figure 2. (a) Plot of predicted value vs. observed value for adsorption of TSPP. (b) Plot of residuals versus predicted response for adsorption of porphyrin. (c) Standardized main effect Pareto chart for the CCD. The vertical line in the chart defines 95% confidence level

$$y=911.0+225.8X_1-25.95X_2+2238X_3-25.07X_4+566.7X_1X_3+3.125X_1X_4+15.83X_1^2+0.4536X_3^2+0.9893X_4^2 \quad (4)$$

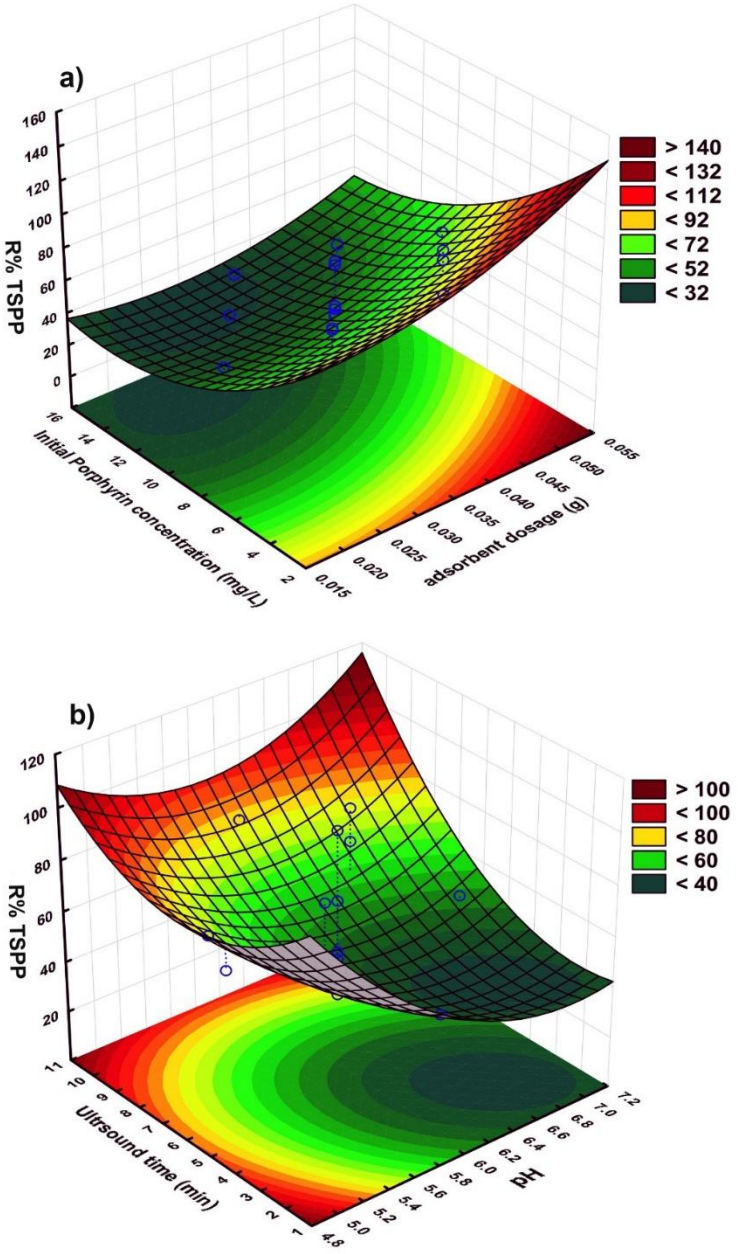

Figure 3. 3D surface mapping plots for multiple effects of (**a**) adsorbent dosage and initial TSPP concentration, (**b**) ultrasound time and pH.

Plot of observed experimental data versus those obtained from Eq. 4 is shown in Fig. 2a. The figure proves that the response predicted according to empirical model is in good agreement with the experimental data. Fig. 2b depicts the diagram of the residuals based on the predicted response percent efficiency. The Pareto chart is used widely in quality control settings to identify critical factors leading to failure or defects in a process (Rosales *et al.*, 2012). In this chart, there is a vertical line that represents a 95% test for significance effect. Passage of each parameters level from vertical critical line proof its significant contribution on response.

In this study, the Pareto chart obtained for adsorption of TSPP (Fig. 2c) shows that all the effects and interactions except the interaction of X_1X_2, X_2X_3, X_2X_4 and X_3X_4 are significant at 95% confidence level.

3.3. Effect of process variables

Fig. 2 (a, b) represents the most relevant fitted response surfaces for the design and depicts the response surface plots of R% versus significant variables. These plots were obtained for a given pair of factors at fixed and optimal values of other variables. Fig. 3 (a) presents the interaction of TSPP concentration with adsorbent dosage. The actual amount of adsorbed TSPP significantly increased. The decrease in the extent of adsorption with initial TSPP concentration was due to the increase in the ratio of the porphyrin molecule to the surface area available for adsorption. These results might be due to the non-availability of active sites on the adsorbent surface.

As shown in Fig. 3 (b), at higher pH a lower adsorption efficiency was observed while more sonication time cause better and higher removal efficiency.

3.4. Numerical optimization of decolorization process

The profile for predicted values and desirability option in the statistical 10.0 software is used to optimize the process (Fig. 4). The scale in the range of 0.0 (undesirable) to 1.0 (very desirable) issued to judgment value for global function (DF) as best criterion for optimization of designed variables.

The CCD (Table 1) has maximum (96.00%) and minimum (30.00%) R% for TSPP and their analysis of 1.0 is related to maximum removal percentage (98.16%) is assigned to following best mild conditions: 0.04 g of Cu-NW-AC, 6 mg l^{-1} of TSPP in pH=5.5 and ultrasound time of 8.0 minutes at room temperature.

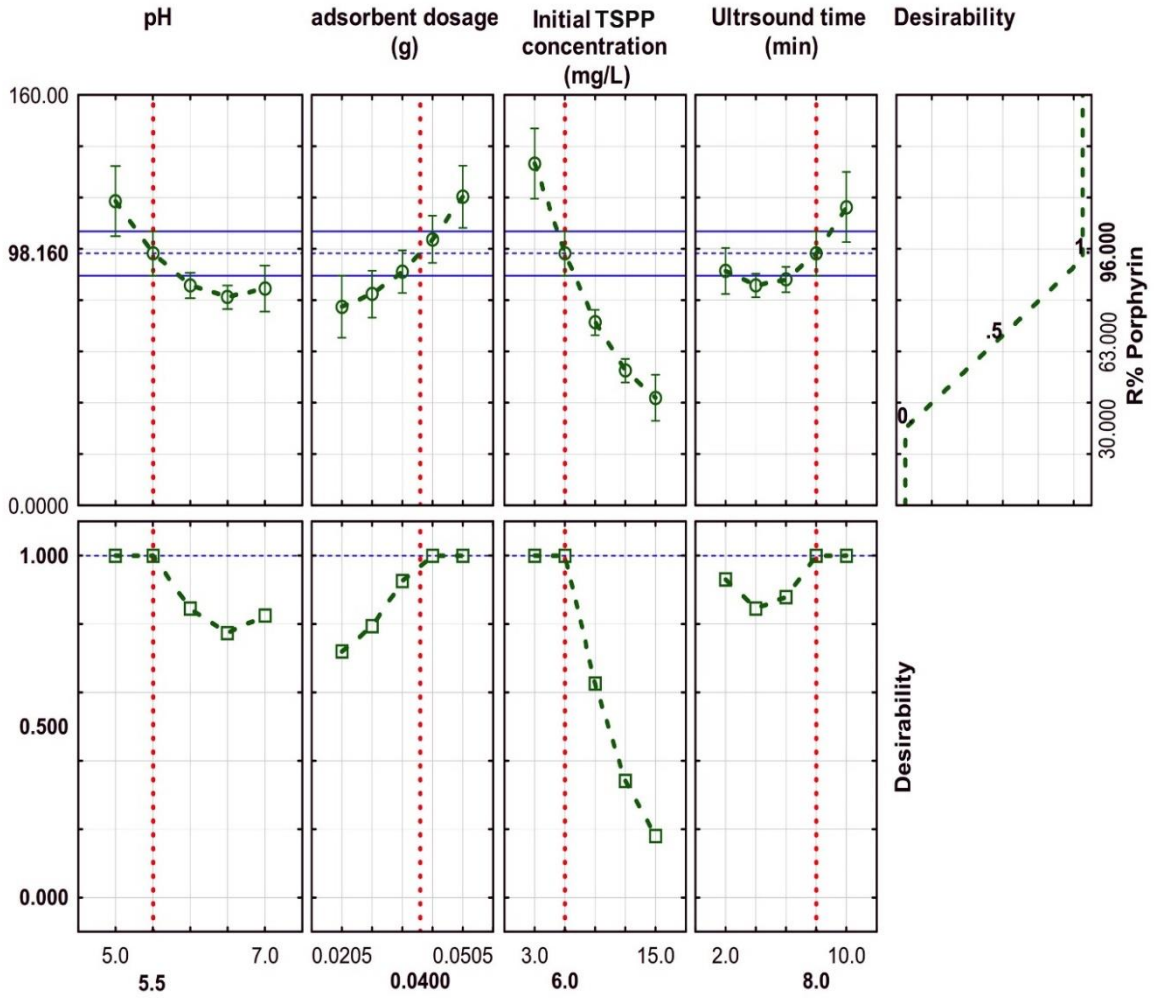

Figure 4. Profiles for predicated values and desirability function for adsorption of TSPP. Dashed line indicated current values after optimization.

3.5. Isotherm study

Adsorption equilibrium isotherms represent mathematical relation of amount of adsorbed target per gram of adsorbent (q_e (mg g^{-1})) to the equilibrium solution concentration (C_e; mg l^{-1}) at fixed temperature. This investigation has great attention from both theoretical and practical point of view to obtain strong knowledge about surface properties of adsorbent and removal mechanism (Asfaram *et al.*, 2015b).

The experimental adsorption equilibrium data for adsorption mechanism on to Cu-NWs-AC was evaluated using different models such as Langmuir, Freundlich, Temkin, Dubinin-Radushkevich methods.

The Langmuir isotherm validity and applicability is correspond to situations such as solute adsorption as monolayer identical surface sites through similar energies without transmigration (Langmuir, 1916). The maximum adsorption capacity is criterion for judgment about suitability of adsorbent for real situation (Oberle *et al.*, 2015).

A plot of C_e/q_e versus C_e should indicate a straight line with slope of $1/Q_m$ and an intercept is equal to $1/(K_aQ_m)$ (Table 3).

The high adsorption capacity of 26.385 mg g^{-1} using 0.035-0.04 g adsorbent shows that the equilibrium data correspond to TSPP adsorption follow the Langmuir model (Table 3).

The Freundlich model (Ghaedi *et al.*, 2015b) is assigned to adsorption onto non-ideal heterogeneous sites following logarithmic decrease in process enthalpy.

k_F show information about the binding energy (adsorption or distribution coefficient) and also quantity of adsorbed dye, while1/n show adsorption intensity of TSPP onto the adsorbent (surface heterogeneity)

The value closer to zero confirms the heterogeneity of surface. 1/n < 1 indicates normal Langmuir isotherm while 1/n above 1 indicate bi-mechanism and cooperative adsorption). The applicability of the Freundlich adsorption isotherm was assessed by plotting log (q_e) versus log (C_e) and respective values for these model constants is shown in Table 3. The correlation coefficients (0.987-0.989) show that Freundlich model has lower efficiency with respect to Langmuir model.

Temkin adsorption isotherm judgment is carried out according to R^2 value and lower value is concerned to error analysis (Abdallah & Taha, 2012). Although, both Langmuir and Freundlich model has reasonable and acceptable for R^2 value, but they assume that heat is logarithmic relation in contrast to adsorption.

In this model, B is the Temkin constant related to heat of the adsorption (J mol^{-1}), T is the absolute temperature (K), R is the universal gas constant (8.314 J mol^{-1} k^{-1}) and K_T is the equilibrium binding constant (L mg^{-1}).

Examination of the data shows that the Temkin isotherm is efficiently usable for fitting the TSPP adsorption onto Cu-NWs-AC. The linear isotherm constants and coefficients of determination are presented in Table 3. The heat of TSPP adsorption onto Cu-NWs-AC was found to increase from 3.346 to 4.783 kJ mol^{-1} with decrease in Cu-NWs-AC from 0.035 to 0.04 g. The correlation coefficients R^2 obtained from Temkin model were comparable to that of Langmuir and Freundlich equations, which explain the applicability of Temkin model to the adsorption of TSPP onto Cu-NWs-AC.

The Dubinin-Radushkevich (D-R) model was also applied to estimate the porosity, free energy and the characteristics of adsorbents (Chieng *et al.*, 2015). The D-R isotherm does not assume a homogeneous surface or constant adsorption potential.

In this model, K is a constant related to the adsorption energy, Q_S is the theoretical saturation capacity, ε is the Polanyi potential. The slope of the plot of ln q_e versus ε^2 gives K (mol^2 $(kJ^2)^{-1}$) and the intercept yields the adsorption capacity; Q_S (mg g^{-1}). The mean free energy of adsorption (E), for transfer of one mole of the target from infinity in solution to the surface of the solid was calculated from the K value using the following relation (Lakouraj *et al.*, 2015):

$$E=\frac{1}{\sqrt{2K}} \tag{5}$$

The calculated value of D-R parameters is given in Table 3. The model saturation adsorption capacity at optimum conditions using different amount of adsorbents (0.035-0.04 g) is in good agreement with respective Langmuir value (26.385-15.698 mg g^{-1}).

This models was applied in two dosage of adsorbent at optimal condition and the results are reported in Table 3. Fitting the experimental data in these isotherm models and considering the higher values of correlation coefficients (R^2 =0.999) it is concluded that Langmuir isotherm model is the best model to explain the TSPP adsorption over Cu-NWs-AC.

Table 3. Isotherm constant parameters and correlation coefficients calculated for the adsorption of TSPP onto Copper nanowires-AC.

Isotherm	Equation	Parameters	0.035	0.04 g
Langmuir	$1/q_e = 1/(K_a Q_m Ce) + 1/Q_m$	Q_m (mg g^{-1})	26.385	15.698
		K_a (l mg^{-1})	0.801	1.810
		R^2	0.995	0.996
Freundlich	$q_e = \ln K_F + (1/n) \ln C_e$	1/n	0.750	0.595
		K_F (l mg^{-1})	2.953	2.764
		R^2	0.990	0.987
Temkin	$q_e = B_1 \ln KT + B_1 \ln C_e$	B_1	4.783	3.346
		K_T(l mg^{-1})	10.927	19.283
		R^2	0.984	0.987
Dubinin-radushkevich	$\ln q_e = \ln Q_s - B\varepsilon^2$	Q_s (mg g^{-1})	13.135	10.665
		$\beta \times 10^{-8}$	5.850	3.960
		E (kJ mol^{-1})	4.135	5.025
		R^2	0.977	0.975

3.6. Kinetic study

Several steps explain dynamics and mechanism of sorption process such as chemical reaction, diffusion control and mass transfer. Thus, pseudo-first-order (Ho, 2006), pseudo-second-order (Lagergren, 1898), Elovich (Aksakal & Ucun, 2010) and intraparticle diffusion (Asfaram *et al.*, 2014) kinetic models were used to analyze the adsorption of TSPP onto Cu-NWs-AC. The agreement between experimental data and the model-predicted values usually need high correlation coefficients (R^2 values close or equal to 1). The relatively higher value shows the more applicability of model and closeness of experimental and theoretical adsorption capacity.

In pseudo-first-order model, plot of log (q_e-q_t) versus t gives a linear relationship from which k_1 and q_e can be determined from the slope and intercept, respectively. If the intercept dose not equal q_e then the reaction is not likely to be first-order reaction even this plot has high correlation coefficient with the experimental data (Rahman & Haseen, 2014). The variation in rate should be proportional to the first power of concentration for strict surface adsorption. However, the relationship between initial solute concentration and rate of adsorption will not be linear when pore diffusion limits the adsorption process.

The correlation coefficient R^2 is relatively low for most adsorption data (Table 4), which indicates that the adsorption of TSPP onto Cu-NWs-AC. The adsorption kinetic may be described by the pseudo-second order model. the plots of log (q_e–q_t) versus *t* does not show good results for the entire sorption period, the plots of t/q_t versus t give straight line confirm the applicability of the pseudo-second-order equation. Values of k_2 and q_e (calculated from the intercept and slope of the plots of t/q_t versus t*)* and R^2 value, in addition to closeness of q_e experimental to theoretical value indicate that this equation produced better results (Table 4): R^2 values for pseudo-second-order kinetic model were found to be higher (0.999) for Cu-NWs-AC, and the calculated q_e values are mainly equal to the experimental data. This indicates that the TSPP adsorption systems obey the pseudo-second-order kinetic model for the entire sorption period.

Table 4. Kinetic parameters for the adsorption of dyes using 0.035 and 0.04 g Copper nanowires-AC as well as 6 mg l^{-1} of TSPP.

	Equation	Value of parameters		
Model		Parameters	0.035 g	0.04 g
Pseudo-First-order- kinetic	$\log (q_e-q_t) = \log (q_e) - k_1/2.303t$	k_1 (min^{-1})	0.572	0.463
		$q_{e\ (calc)}$ (mg g^{-1})	2.914	1.010
		R^2	0.924	0.968
Pseudo-second-order-kinetic	$(t/q_t) = 1/(k_2q_e^2) + 1/q_e(t)$	k_2 (min^{-1})	0.003	0.001
		$q_{e\ (calc)}$ (mg g^{-1})	9.804	9.900
		R^2	0.999	0.999
Intraparticle diffusion	$q_t = K_{dif}\ t^{1/2} + C$	K_{diff} (mg g^{-1} $min^{-1/2}$)	0.812	0.394
		C (mg g^{-1})	7.513	8.805
		R^2	0.991	0.999
Elovich	$q_t = 1/\beta \ln(\alpha\beta) + 1/\beta \ln(t)$	β (mg g^{-1} min^{-1})	1.548	0.316
		α (g mg^{-1})	25.102	681.33
		R^2	0.957	0.982
	Experimental data	$q_{e\ (exp)}$ (mg g^{-1})	9.558	9.772

The Elovich equation is another rate equation based on the adsorption capacity. In this model, plot of q_t versus ln (t) should yield a linear relationship if the Elovich is applicable with a slope of (1/β) and intercept of (1/β) ln (αβ) (Ghaedi *et al.*, 2015c). The Elovich constants obtained from the slope and the intercept of the straight line reported in Table 4.

Another alternative method for kinetic evaluation of an adsorption process is intra-particle-diffusion. In this process TSPP is probably transported from its aqueous solution to the adsorbents by intraparticle diffusion. Therefore, this model should be used to study the rate-limiting step for both dyes adsorption onto Cu-NWs-AC.

The values of K_{dif} and C (calculated from the slopes of q_t versus $t^{1/2}$) value is reported in Table 4. The values of q_t were found to give two lines part with values of $t^{1/2}$ and the rate constant K_{dif} directly evaluated from the slope of the second regression line. Two lines depend to the exact mechanism; the first one of represent initial surface adsorption and the second one is the intraparticle diffusion at the end of the reaction. As still there is no sufficient indication about which of the two steps is the rate-limiting step.

It was reported that if the intraparticle diffusion is the sole rate-limiting step, the plot of q_t versus $t^{1/2}$ must pass through the origin and the value of C is equal to zero. Both of these results show that the intraparticle diffusion model may be the controlling factor in determining the kinetics of the process (Dahri *et al.*, 2014). The R^2 a value given in Table 4 is away to unity show not applicability of this model and, reject that the rate-limiting step is the intraparticle diffusion process. In this case, the intraparticle diffusion model may be the controlling factor in determining the kinetics of the process.

4. Conclusion

The Cu-NWs-AC with high surface area were synthesized in our research lab and characterized with SEM and XRD analysis. This material successfully used for adsorption of meso-tetrakis(4-sulfonatophenyl)porphyrin (TSPP) as an organic dye in aqueous solution by spectrophotometry. By using RSM, the effective pH was found to be 5.5 and the optimum adsorbent dose was found to be 0.040 g for 6.0 mg l^{-1} of TSPP at 8.0 min ultrasound time with removal percentage above 98.00%. The predictions of the model are in good agreement with the experimental data and the evaluation tests demonstrate that

the regression model produced by RSM is reliable in the range of operating conditions. This DOE technique is a proper method to maximize the adsorption by estimating the optimum operating parameters. Langmuir isotherm gave best fit to adsorption data compared to other isotherms. This fact may be attributed to high Langmuir surface area of the adsorbent. The data indicated that the adsorption kinetics follows the pseudo-second-order rate in addition to intraparticle diffusion.

Acknowledgment

The authors express their appreciation to Yasouj University Research Council for financial support of this work.

References

Abdallah R. and Taha S. (2012), Biosorption of methylene blue from aqueous solution by nonviable *Aspergillus fumigatus*, *Chem. Eng. J.*, **195–196**, 69-76.

Aksakal O. and Ucun H. (2010), Equilibrium, kinetic and thermodynamic studies of the biosorption of textile dye (Reactive Red 195) onto *Pinus sylvestris L.*, *J. Hazard. Mater.*, **181**, 666-672.

Asfaram A., Fathi M., Khodadoust S. and Naraki M. (2014), Removal of Direct Red 12B by garlic peel as a cheap adsorbent: Kinetics, thermodynamic and equilibrium isotherms study of removal, *Spectrochim. Acta Part A*, **127**, 415-421.

Asfaram A., Ghaedi M., Goudarzi A. and Rajabi M. (2015a), Response surface methodology approach for optimization of simultaneous dye and metal ion ultrasound-assisted adsorption onto Mn doped Fe_3O_4-NPs loaded on AC: kinetic and isothermal studies, *Dalton Trans.,* **44**, 14707-14723.

Asfaram A., Ghaedi M., Agarwal S., Tyagi I. and Kumar Gupta V. (2015b), Removal of basic dye Auramine-O by ZnS:Cu nanoparticles loaded on activated carbon: optimization of parameters using response surface methodology with central composite design, *RSC Adv.*, **5**, 18438-18450.

Bagheri A.R., Ghaedi M., Hajati S., Ghaedi A.M., Goudarzi A. and Asfaram A. (2015), Random forest model for the ultrasonic-assisted removal of chrysoidine G by copper sulfide nanoparticles loaded on activated carbon; response surface methodology approach, *RSC Adv.,* **5**, 59335-59343.

Chieng H.I., Lim L.B. and Priyantha N. (2015), Enhancing adsorption capacity of toxic malachite green dye through chemically modified breadnut peel: equilibrium, thermodynamics, kinetics and regeneration studies, *Environ. Technol*, **36**, 86-97.

Chow J.H. and Chow C. (2006), *The Encyclopedia of Hepatitis and Other Liver Diseases*. Infobase Publishing.

Dahri M.K., Kooh M.R.R. and Lim L.B. (2014), Water remediation using low cost adsorbent walnut shell for removal of malachite green: equilibrium, kinetics, thermodynamic and regeneration studies, *J. Environ. Chem. Eng.,* **2**, 1434-1444.

De Montellano P.R.O. (2005), *Cytochrome P450: structure, mechanism, and biochemistry*. Springer Science & Business Media.

Duran A., Tuzen M. and Soylak M. (2009), Preconcentration of some trace elements via using multiwalled carbon nanotubes as solid phase extraction adsorbent, *J Hazard. Mater.*, **169**, 466-71.

Fayyazi E., Ghobadian B., Najafi G., Hosseinzadeh B., Mamat R. and Hosseinzadeh J. (2015), An ultrasound-assisted system for the optimization of biodiesel production from chicken fat oil using a genetic algorithm and response surface methodology, *Ultrason Sonochem*, **26**, 312-20.

Feiters M.C., Rowan A.E. and Nolte R.J. (2000), From simple to supramolecular cytochrome P450 mimics, *Chem. Soc. Rew.,* **29**, 375-384.

Ghaedi M., Shojaeipour E., Ghaedi A.M. and Sahraei R. (2015a), Isotherm and kinetics study of malachite green adsorption onto copper nanowires loaded on activated carbon: artificial neural network modeling and genetic algorithm optimization, *Spectrochim. Acta Part A,* **142**, 135-49.

Ghaedi M., Khajehsharifi H., Yadkuri A.H., Roosta M. and Asghari A. (2012a), Oxidized multiwalled carbon nanotubes as efficient adsorbent for bromothymol blue, *Toxicol. Environ. Chem.*, **94**, 873-883.

Ghaedi M., Tavallali H., Sharifi, M., Kokhdan S.N. and Asghari A. (2012b), Preparation of low cost activated carbon from Myrtus communis and pomegranate and their efficient application for removal of Congo red from aqueous solution, *Spectrochim. Acta Part A,* **86**, 107-114.

Ghaedi M., Hajati S., Zare M., Zare M. and Shajaripour Jaberi S.Y. (2015b), Experimental design for simultaneous analysis of malachite green and methylene blue; derivative spectrophotometry and principal component-artificial neural network, *RSC Adv.,* **5**, 38939-38947.

Ghaedi M., Sadeghian B., Pebdani A.A., Sahraei R., Daneshfar A. and Duran C. (2012c), Kinetics, thermodynamics and equilibrium evaluation of direct yellow 12 removal by adsorption onto silver nanoparticles loaded activated carbon, *Chem. Eng. J.,* **187**, 133-141.

Ghaedi M., Rozkhoosh Z., Asfaram A., Mirtamizdoust B., Mahmoudi Z. and Bazrafshan A.A. (2015c), Comparative studies on removal of Erythrosine using ZnS and AgOH nanoparticles loaded on activated carbon as adsorbents: Kinetic and isotherm studies of adsorption, *Spectrochim. Acta Part A,* **138**, 176-186.

Granville D., McManus B. and Hunt D. (2001), Photodynamic therapy: shedding light on the biochemical pathways regulating porphyrin-mediated cell death, *Histol. Histopathol.*, **16**, 309-317.

Ho Y.-S. (2006), Second-order kinetic model for the sorption of cadmium onto tree fern: a comparison of linear and non-linear methods, *Water Res.*, **40**, 119-125.

Jamshidi M., Ghaedi M., Dashtian K., Ghaedi A.M., Hajati S., Goudarzi A. and Alipanahpour E. (2016), Highly efficient simultaneous ultrasonic assisted adsorption of brilliant green and eosin B onto ZnS nanoparticles loaded activated carbon: Artificial neural network modeling and central composite design optimization, *Spectrochim. Acta Part A*, **153**, 257-267.

Lagergren S. (1898), About the theory of so-called adsorption of soluble substances, *Kungliga Svenska Vetenskapsakademiens Handlingar*, **24**, 1-39.

Lakouraj M.M., Norouzian R.-S. and Balo S. (2015), Preparation and Cationic Dye Adsorption of Novel Fe3O4 Supermagnetic/Thiacalix[4]arene Tetrasulfonate Self-Doped/Polyaniline Nanocomposite: Kinetics, Isotherms, and Thermodynamic Study, *J. Chem. Eng. Data*, **60**, 2262-2272.

Langmuir I. (1916), The constitution and fundamental properties of solids and liquids. Part I. Solids, *J. Am. Chem. Soc.,* **38**, 2221-2295.

Meunier B. (1992), Metalloporphyrins as versatile catalysts for oxidation reactions and oxidative DNA cleavage, *Chem. Rev.*, **92**, 1411-1456.

Nasiri Azad F., Ghaedi M., Dashtian K., Hajati S., Goudarzi A. and Jamshidi M. (2015), Enhanced simultaneous removal of malachite green and safranin O by ZnO nanorod-loaded activated carbon: modeling, optimization and adsorption isotherms, *New J. Chem.*, **39**, 7998-8005.

Oberle M., Yigit C., Angioletti-Uberti S., Dzubiella J. and Ballauff M. (2015), Competitive protein adsorption to soft polymeric layers: binary mixtures and comparison to theory, *J. Phys. Chem. B.,* **119**, 3250-8.

Place D.A., Faustino P.J., Berghmans K.K., van Zijl P.C., Chesnick A.S. and Cohen J.S. (1992), MRI contrast-dose relationship of manganese (III) tetra (4-sulfonatophenyl) porphyrin with human xenograft tumors in nude mice at 2.0 T, *Magn. Reson. Imaging*, **10**, 919-928.

Rahman N. and Haseen U. (2014), Equilibrium Modeling, Kinetic, and Thermodynamic Studies on Adsorption of Pb (II) by a Hybrid Inorganic–Organic Material: Polyacrylamide Zirconium (IV) Iodate, *Ind. Eng. Chem. Res.*, **53**, 8198-8207.

Roosta M., Ghaedi M., Sahraei R. and Purkait M.K. (2015), Ultrasonic assisted removal of sunset yellow from aqueous solution by zinc hydroxide nanoparticle loaded activated carbon: Optimized experimental design, *Mater. Sci. Eng. C, Mater. Biol. Appl.,* **52**, 82-9.

Rosales E., Sanroman M.A. and Pazos M. (2012), Application of central composite face-centered design and response surface methodology for the optimization of electro-Fenton decolorization of Azure B dye, *Environ. Sci. Pollut. Res. Int.*, **19**, 1738-46.

Seufert K., Bocquet M.-L., Auwärter W., Weber-Bargioni A., Reichert J., Lorente N. and Barth J.V. (2011), Cis-dicarbonyl binding at cobalt and iron porphyrins with saddle-shape conformation, *Nature chem.*, **3**, 114-119.

Srivastava T.S. and Tsutsui M. (1973), Unusual metalloporphyrins. XVI. Preparation and purification of tetrasodium meso-tetra (p-sulfophenyl) porphine. Easy procedure, *J. Org. Chem.,* **38**, 2103-2103.

Vicente M. (2001), Porphyrin-based sensitizers in the detection and treatment of cancer: recent progress, *Curr. Med. Chem. Anticancer. Agents,* **1**, 175-194.

Xue B., Sun T., Wu J.K., Mao F. and Yang W. (2015), AgI/TiO_2 nanocomposites: ultrasound-assisted preparation, visible-light induced photocatalytic degradation of methyl orange and antibacterial activity, *Ultrason. Sonochem.*, **22**, 1-6.

Zhou X.-T., Ji H.-B., Cheng Z., Xu J.-C., Pei L.-X. and Wang L.-F. (2007), Selective oxidation of sulfides to sulfoxides catalyzed by ruthenium (III) meso-tetraphenylporphyrin chloride in the presence of molecular oxygen, *Bioorg. Med. Chem. Lett.,* **17**, 4650-4653.